THEORETICAL STUDY ON THE POST-LOCAL BUCKLING OF STEEL PLATES IN CONCRETE-FILLED BOX COLUMNS

Q.Q. Liang[a,*] and **B. Uy**[b]

[a] School of the Built Environment, Victoria University of Technology,
PO Box 14428, Melbourne City MC, VIC 8001, Australia
[b] School of Civil and Environmental Engineering, The University of New South Wales,
Sydney, NSW 2052, Australia

Abstract

This paper presents a theoretical study on the post-local buckling behaviour of steel plates in welded steel box columns filled with concrete by using the finite element method. The effects of various geometric imperfections, residual stresses and width-to-thickness ratios on the post-local buckling characteristics of steel plates in composite columns are investigated. A novel method is developed for evaluating the initial local buckling loads and post-local buckling reserve strength of steel plates with imperfections associated with a theoretical analysis. Two effective width formulas are proposed for the design of clamed steel plates restrained by concrete and are employed in the ultimate strength calculation of short concrete-filled steel box columns. The proposed design models are compared with existing experimental results with a good agreement.

Keywords: Composite columns, concrete, effective width, finite element analysis, post-local buckling, steel plates

* Corresponding author

1. INTRODUCTION

Concrete-filled thin-walled box columns fabricated with thin steel plates have gained popularity in supporting heavy loads in tall buildings, bridges and offshore structures. In a composite column, the concrete is fully encased by the steel box so that the ductility of the concrete stress-strain response is improved. In addition, the steel plates are restrained by the concrete core, which increases the resistance of plates to local buckling. The advantages of composite columns are also related to their cost savings and ability to provide rapid construction. During tall building construction, hollow steel columns can be filled with concrete at the lower levels of the building while steel elements are fabricated at higher levels. Since the construction speed of this structure is increased, the construction cost can be greatly reduced.

The post-local buckling behaviour and strength of rectangular plates subjected to edge compression has been investigated by several researchers. Steel plates with built-in edges under edge compression were reported by Levy [1], who gave an exact solution of von Karman's equations. Coan [2] extended Levy's method to study the post-local buckling of simply supported plates with small initial deflections. Yamaki [3] produced an important paper describing the post-local buckling behaviour of clamped elastic steel plates with initial deflections. Crisfield [4] has undertaken a full-range analysis of steel plates and stiffened plating under uniaxial compression. The ultimate strength of simply supported plates with geometric and material nonlinearities has been reported by Little [5]. Mofflin and Dwight [6] have described the buckling behaviour of aluminium plates with geometric imperfections and residual stresses.

More recently, Ge and Usami [7,8] have investigated the local buckling and strength of concrete-filled thin-walled steel box columns. Wright [9,10] has presented theoretical studies on the local buckling of steel plates in contact with concrete and derived the maximum width-to-thickness ratios for plates based on an energy approach. Bridge *et al.* [11] has undertaken tests on the local buckling of square thin-walled steel tubes with concrete infill. Furthermore, Uy and Bradford [12,13] have conducted theoretical and experimental investigations on the local buckling of steel plates in composite steel-concrete members. However, the post-local buckling characteristics of steel plates with geometric imperfections and residual stresses in concrete-filled welded thin-walled box columns have not been adequately studied theoretically, and there is also lack of an efficient method for evaluating the initial local buckling loads of steel plates with imperfections.

This paper presents a theoretical study on the post-local buckling behaviour of steel plates in concrete-filled welded thin-walled box columns based on the finite element method. The treatments of initial geometric imperfections and residual stresses are discussed herein. The finite element model developed is initially compared with the post-local buckling results given by Yamaki [3] for clamped steel plates with initial deflections. Numerical studies are then carried out to investigate the effects of various initial geometric imperfections, residual stresses, and width-to-thickness ratios on the post-local buckling behaviour of clamped steel plates restrained by concrete. The novel method developed herein is employed to determine the initial local buckling loads of steel plates with imperfections. An effective width model is proposed for the ultimate strength design of clamped steel plates restrained by concrete and of short concrete-filled welded box columns in compression. Finally, the proposed design models are verified by the existing experimental results.

2. OUTLINE OF FINITE ELEMENT ANALYSIS

2.1 Finite element model

The post-local buckling behaviour of steel plates in concrete-filled welded box columns was investigated by using the finite element analysis program STRAND6.1 [14]. The local buckling displacements of plates were described by using an eight-node quadratic plate element developed based on the Mindlin plate theory. The plate was discretised into 10×10 mesh as it was found that the quadratic element and the mesh used were sufficient to describe the local buckling mode and give a good degree of accuracy based on a sensitivity analysis. The plasticity of steel plates was treated by adopting the von Mises yield criterion with a volume approach incorporating 10 layers. A clamped boundary condition was assumed for the four edges of the plate to represent a half-wave in the buckled shape of a flange of a concrete-filled thin-walled box column, which is buckling locally.

2.2 Treatments of geometric imperfections and residual stresses

The initial geometric imperfections of steel plates in concrete-filled welded box columns are usually induced during the process of manufacture, welding and construction. The initial geometric imperfection that has the same half-wavelength as the local buckling mode was considered in the analysis as illustrated in Fig. 1. In the present study, a small lateral pressure applied to the surface of the plate was used to represent the initial geometric imperfections. The magnitude of the lateral pressure was determined by undertaking a linear static analysis of the model under a trial loading, which causes the maximum deflection at the centre of the plate equal to the specified geometric imperfection. The lateral pressure was applied throughout the load increments to ensure the plate remain deflected in the nonlinear finite element analysis.

The process of welding causes a complex state of temperature and stress distribution with time in a welded steel plate. Tensile residual stresses are induced in the region of the weld whilst compressive residual stresses are present in the remainder of the plate. It is confirmed experimentally that compressive residual stresses in the cross section of the plate are balanced by the tensile residual stresses that reach the yield stress of the steel plate. Dwight [15] has reported the distribution of residual stresses within a welded plate of a steel box column. An idealised residual stress pattern in a concrete-filled welded thin-walled box column is shown in Fig. 2 where residual stresses have been adjusted to suit the finite element mesh. Residual stresses were treated as a pre-load that was combined with the applied edge stresses in the analysis.

2.3 Material stress-strain curve

The material stress-strain behaviour of steel plates in a concrete-filled welded thin-walled box column is affected by residual stresses. When the sum of the applied stress and the compressive residual stress acting on the part of the welded plate is equal to the yield stress of the metal, yielding will occur. After yielding, the material stress-strain behaviour of the welded steel plate is no longer analogous to that of a tensile test coupon without residual stresses. A typical material stress-strain curve of a welded steel plate with residual stresses is illustrated in Fig. 3. It is clear that a welded plate displays a rounded stress-strain form that differs from the tensile test behaviour of a coupon without residual stresses.

The formula suggested by Ramberg-Osgood [16] was employed to define the rounded stress-strain curve of steel plates with residual stresses in the present analysis. The Ramberg-Osgood formula is expressed by

$$\varepsilon = \frac{\sigma}{E}\left[1 + \frac{3}{7}\left(\frac{\sigma}{\sigma_{0.7}}\right)^n\right] \tag{1}$$

in which σ and ε are uniaxial stress and strain respectively, E is the Young's modulus, $\sigma_{0.7}$ is the secant yield strength, which is the stress corresponding to $E_{0.7} = 0.7E$, and n is the knee factor that defines the sharpness of the knee of the material stress-strain curve. It has been found that the knee factor n = 25 can be used in Equation (1) to express the material stress-strain behaviour of steel plates with residual stresses and provides sufficient accurate results for use in engineering practice [6].

3. COMPARISON WITH CLASSICAL SOLUTION

Before investigating the post-local buckling strength of steel plates in concrete-filled thin-walled box columns, the model developed was used to analyse a clamped elastic steel plate with initial deflections, and the results were compared with the classical postbuckling solution provided by Yamaki [3]. In the present finite element analysis, the initial transverse deflection of $0.1t$ was incorporated in the plate that was divided into a 10×10 mesh, and the Poisson's ratio was taken as 1/3 as used by Yamaki. A comparison of results obtained from the present study with Yamaki's postbuckling results is shown in Fig. 4, in which the load factor is denoted as $\beta = \sigma_a (b/t)^2 / \pi^2 E$, where σ_a is the applied edge stress and b and t are the width and thickness of the plate respectively. It can be concluded from the results that the present finite element analysis gives very good agreement with the classical solution, and the representation of initial geometric imperfections by using the lateral pressure is a suitable method.

4. NUMERICAL STUDIES

4.1 Plates with various geometric imperfections

Clamped steel plates in concrete-filled box columns with various initial geometric imperfections were analysed in order to evaluate the effects of initial imperfections on the post-local buckling behaviour and strength of plates. Square slender plates with b/t = 100 and the geometric imperfections of $0.1t$~$0.5t$ were studied. The material properties of the plates considered in this study are: the proof stress $\sigma_{0.2}$ = 300 MPa, compressive residual stress $\sigma_r = 0.25\sigma_{0.2}$, and the Young's modulus E = 200,000 MPa. The load-transverse deflection, load-edge shortening and load-strain curves obtained from the finite element analysis are illustrated in Figs. 5 to 7, respectively. The elastic critical local buckling stress σ_{cr} of perfect steel plates was determined by using the expression given by Bulson [17] as

$$\sigma_{cr} = \frac{k\pi^2 E}{12(1-v^2)\left(\frac{b}{t}\right)^2} \quad (2)$$

in which v is the Poisson's ratio and k is the elastic local buckling coefficient which depends on the aspect ratio and the boundary condition of the plate. The minimum elastic local buckling coefficient for clamped perfect plates used in this study was 9.81 which was obtained by undertaking a linear finite element buckling analysis of plates based on the bifurcation buckling theory.

It can be observed from Fig. 5 that the total and net central transverse deflections increase with an increase in initial deflections under the same loading. The load-carrying capacity of plates decreases with an increase in initial deflections and plates with larger initial imperfections have lower ultimate strength. Figure 6 indicates that initial local buckling reduces the stiffness of plates, and the post-local buckling stiffness decreases with an increase in initial imperfections. The central strains in the loading direction shown in Fig. 7 are also reduced by an increase in initial imperfections. Due to the shortening of the postbuckling half-wavelength, the central strain displays reversal after reaching the maximum value.

4.2 Plates with various residual stresses

The effects of residual stresses on the post-local buckling behaviour of steel plates with the slenderness values of b/t = 40, 70 and 100 in concrete-filled welded box columns were studied by varying the compressive residual stress levels. The compressive residual stresses of $\sigma_r = 0$, $\sigma_r = 0.125\sigma_{0.2}$ and $\sigma_r = 0.25\sigma_{0.2}$ were used to represent the conditions of stress relieved, lightly welded and heavily welded plates, respectively. Initial geometric imperfections of $0.1t$ were considered in the analysis of all plates.

Figure 8 presents the load-edge shortening curves of clamped plates with various residual stresses obtained from the finite element analysis. It can be observed that residual stresses have a more pronounced effect on stocky and compact plates that will yield at a lower stress due to the presence of compressive residual stresses. In addition, the stiffness of plates decreases with an increase in compressive residual stresses. Moreover, the ultimate strength of plates is reduced by the presence of residual stresses and this decreases with the increase of compressive residual stresses. However, the post-local buckling behaviour of slender plates is not extremely sensitive to the presence of residual stresses as yielding generally doesn't occur prior to local instability.

4.3 Plates with various width-to-thickness ratios

In order to determine the post-local buckling strength of steel plates in the different forms of concrete-filled box columns, it is essential to analyse plates with various width-to-thickness ratios. In the present study, clamped steel plates with a range of *b/t* ratios from 30 to 110 were analysed. Since geometric imperfections and residual stresses are usually present in welded steel box columns filled with concrete, the initial imperfections of $w_0 = 0.1t$ and residual compressive stresses of $\sigma_r = 0.25\sigma_{0.2}$ were incorporated in the analysis.

The load-transverse deflection curves of clamped steel plates with various *b/t* ratios obtained from the analysis are summarized in Fig. 9. It is evident that the initial local buckling stress and ultimate strength of plates are both reduced by initial geometric imperfections and residual stresses. Plates with larger *b/t* ratios exhibit lower local buckling stress and ultimate strength, and the results for plates with a slenderness ratio *b/t* = 30 and 40 are identical because plates only undergo yielding for these cases.

5. INITIAL LOCAL BUCKLING LOADS OF IMPERFECT PLATES

Due to the presence of initial geometric imperfections, no bifurcation point can be observed on the load-transverse deflection curves of steel plates as shown in Fig. 9. This leads to difficulty in determining the initial local buckling loads of plates with imperfections. Coan [2] suggested that the initial local buckling load of a plate could be determined by locating the inflection point on the load-central transverse deflection plot. The inflection point represents the maximum rate of the increment of transverse deflection with the load. This method, which requires determining the minimum slope of the load-deflection curve, has been found difficult to apply in practice. The load-central axial strain curve has also been employed to evaluate the initial buckling loads of imperfect plates due to the curve having a well-defined break as recommended by Coan. In this approach the vertical tangent of the load-strain curve is usually taken as the criterion of the initial local buckling load for the plate. However, this approach can only be used for isotropic plates and it also generally overestimates the initial local buckling load. Other methods such as a load-edge shortening plot have been used to evaluate the initial local buckling loads of imperfect plates. It has been found that these methods mentioned are either too difficult to be used in practice or inaccurate for determining the initial local buckling loads of plates with initial imperfections.

A novel and simple method for evaluating the initial local buckling loads of plates with geometric imperfections and residual stresses has been developed by the authors based on the load-transverse deflection relations associated with the theoretical analysis. The inflection point can be easily found by plotting the nondimensional central transverse deflection versus the ratio of the deflection to the applied load w/σ_a. The minimum value of w/σ_a determined from the plot represents the inflection point where local buckling occurs at the corresponding loading level. It should be noted that for stocky plates the inflection point might indicate yielding or plastic local buckling because the sudden changes of the configuration of plastic deformations with loads are only related to yielding and plastic local buckling. The translations of load-deflection curves to the transverse deflection versus w/σ_a curves for plates with various initial deflections are shown in Fig. 10. Further results for plates with various *b/t* ratios are presented in Figs. 11 to 14, respectively. Each of these analyses employed initial imperfections of $0.1t$.

It can be observed from the figures that the ratio of w/σ_a decreases with a corresponding increase in load and deflection in the first few loading increments, and after reaching the minimum value, it increases with the increase of load and deflection. This relationship between load and deflection can be explained. Before initial local buckling, the lateral deflections of the plate have a small increase with the applied load. However, after local buckling, deflections increase rapidly even under a small loading increment because local buckling has reduced the stiffness of the plate. If the plate hasn't lost local stability, the deflections will not change rapidly under a small load increment. Therefore, it is clear that the inflection point defined by the minimum ratio of w / σ_a represents the onset of initial local buckling of steel plates with imperfections.

It is worth noting that the proposed method for determining the initial local buckling loads of steel plates with geometric imperfections and residual stresses is different from the Southwell Method, which is used for extrapolating for the elastic critical load of a steel column from test data. The Southwell Plot cannot be used for the interpretation of a plate test because steel plates do not behave in a similar manner to struts as pointed out by Walker [18]. However, the proposed method can also be used to evaluate the initial local buckling loads of steel plates from the experimental measurements of load-deflection responses. Furthermore, it should be noted that the initial local buckling load of a steel plate with geometric imperfections and residual stresses will be less then that of a perfect plate. The elastic critical local buckling load of a flat plate without residual stresses can be simply calculated using Equation (2).

6. POST-LOCAL BUCKLING RESERVE STRENGTH

After initial local buckling, thin steel plates are still capable of carrying much more loads without failure as shown in Fig. 9. The post-local buckling reserve strength of steel plates in concrete-filled thin-walled box columns has been of increasing concern in order to optimise the use of steel. The post-local buckling reserve strength of a plate can be defined as

$$\sigma_P = \sigma_u - \sigma_c \tag{3}$$

where σ_P is the post-local buckling reserve strength, σ_u is the ultimate strength and σ_c is the initial local buckling stress of a plate with imperfections. This initial critical stress can be determined from the results of a theoretical analysis by the novel method described previously.

Table 1 gives the initial local buckling loads, post-local buckling reserve strength and ultimate strength of steel plates (*b/t* = 100) with $\sigma_r = 0.25\sigma_{0.2}$ and various initial imperfections in composite columns. It can be seen that the initial local buckling loads σ_c for plates with initial imperfections are less than that of a perfect plate (σ_{cr}= 177 MPa). However, the interesting fact is that the initial local buckling stress increases with the amplitude of geometric imperfections. This is because a plate with geometric imperfections has been in the state in which its stiffness has been reduced by deflecting out of the plane. It states that the plate with initial imperfections has lost its initial local stability before the load is applied to it. Moreover, Table 1 indicates that the post-local buckling strength of plates with smaller initial imperfections is higher than that of plates with larger ones. The post-local buckling reserve strength of a plate with an initial imperfection of 0.1*t* is 55% of its ultimate strength whilst it is only 28% of the ultimate strength of a plate with an initial imperfection of 0.5*t*.

The initial local buckling loads, post-local buckling reserve strength and the ultimate strength of clamped steel plates with 0.1*t* geometric imperfections and various *b/t* ratios are presented in Table 2. It can be seen that plates with smaller *b/t* ratios possess higher initial local buckling loads, but stocky plates such as *b/t* = 40 and 50 have the same initial local buckling load because under this critical load yielding will occur. In addition, the post-local buckling strength of plates with b/t ratios in the range from 50 to 100 increases with an increase in the *b/t* ratios. For a plate with *b/t* = 50, its post-local buckling reserve strength is 16% of its ultimate strength, but the post-local buckling reserve strength of a plate with *b/t* = 110 will increase to 58% of its ultimate strength. Furthermore, it should be noted that when the *b/t* ratio of plates is greater than 100, their post-local buckling strength will start decreasing due to the shortening of the post-local buckling half-wavelength.

7. EFFECTIVE WIDTH OF PLATES IN CONCRETE-FILLED BOX COLUMNS

It can be seen from Tables 1 and 2 that the post-local buckling reserve strength of thin steel plates is very high. In order to optimise the use of steel, this beneficial post-local buckling strength should be taken into account in design. The present finite element analysis of plates has confirmed that in the post-local buckling regime the two unloaded edge strips of the plate carry most of the load while the heavily buckled central region withstands relatively lower stresses. Therefore, the post-local buckling behaviour of steel plates in concrete-filled box columns can approximately be expressed by the effective width, which can be determined from the results of a nonlinear finite element analysis as

$$\frac{b_e}{b} = \frac{\sigma_u}{\sigma_{0.2}} \tag{4}$$

where b_e is the effective width of the plate.

The effective width of steel plates in concrete-filled welded box columns with a geometric imperfection of $0.1t$ and residual stress of $\sigma_r = 0.25\sigma_{0.2}$ obtained from the finite element analysis is shown in Table 3. Based on these results, two effective width formulas have been proposed by Liang and Uy [19] in a companion paper for the ultimate strength design of steel plates in concrete-filled thin-walled box columns as follows:

$$\frac{b_e}{b} = 0.675\left(\frac{\sigma_{cr}}{\sigma_{0.2}}\right)^{1/3} \tag{5}$$

when $\sigma_{cr} \leq \sigma_{0.2}$, and

$$\frac{b_e}{b} = 0.915\left(\frac{\sigma_{cr}}{\sigma_{cr} + \sigma_{0.2}}\right)^{1/3} \tag{6}$$

when $\sigma_{cr} > \sigma_{0.2}$.

It is seen from above formulas that the effective width of steel plates in concrete-filled box columns is described by the proof stress $\sigma_{0.2}$ or the yield stress of the steel plate and the elastic critical local buckling stress σ_{cr}, which is determined by Equation (2) with a minimum buckling coefficient of 9.81. It is noted that Equations (5) and (6) provide conservative estimates to the finite element results. This is because the proposed formulas have considered that steel plates in real thin-walled concrete-filled box columns may have greater imperfections than the present finite element model.

8. ULTIMATE STRENGTH OF CONCRETE-FILLED STEEL BOX COLUMNS

In a concrete-filled circular tubular column under axial compression, the steel tube usually provides confinement to the infilled concrete core. This confinement effect can enhance the strength of the composite column. However, the confinement effect of steel on the concrete in a concrete-filled rectangular box column is limited to the corners of the section and is very small, which can be negligible in design. Therefore, the ultimate strength of a short concrete-filled rectangular steel box column in compression considering post-local buckling can be calculated by combining the ultimate strength of the concrete core and the steel plates, which is expressed by

$$N_u = 0.85 f_c A_c + f_y A_{se} \tag{7}$$

in which f_c is the compressive cylinder strength of concrete, A_c is the concrete area of the cross section, f_y is the yield stress of the steel plate and A_{se} is the total effective steel area of the cross section which is determined by using the proposed effective width formulas Equations (5) and (6). The uncertainty between the test cylinder strength and in-situ strength of concrete is accounted for by the reduction factor of 0.85.

9. COMPARISON WITH EXPERIMENTAL RESULTS

The proposed design models of effective width for plates and of ultimate strength for concrete-filled steel box columns are compared with existing experimental results in Table

4. Specimens B5~B29 were conducted by Bridge *et al.* [11] while specimens NS1~NS17 were undertaken by Uy [20]. Specimens NS5, NS11, NS17 and B5~B29 were designed to investigate the local buckling strength of plates restrained by concrete so that they were constructed by filling concrete to the welded steel box with 20 or 5 mm gap to the ends of the box. The load was applied to the steel plates only in the test. As a result of this, the proposed effective width model can be compared with these specimens. It can be observed from Table 4 that the theoretical predictions on the ultimate strength of clamped steel plates and of concrete-filled box columns using the proposed design models agree very well with the experimental results. The mean theoretical ultimate strength is 94% of that of the experimental results. Therefore, the proposed effective width formulas can be used in the design of concrete-filled steel box columns and of clamped steel plates in other composite steel-concrete members.

10. FURTHER RESEARCH

The initial local buckling of thin steel plates is not a failure mode since the steel plates can still carry much more increased load without failure. Most of research has been focused on the ultimate strength of steel plates in concrete-filled thin-walled box columns and little work has been undertaken to study the initial local buckling strength of steel plates with imperfections in such columns. The present method herein for determining the initial local buckling loads of steel plates with imperfections seems to provide reasonable results, which are valuable for studying the behaviour of concrete-filled steel box columns. However, it is necessary to undertake further tests on concrete-filled steel box columns to investigate the experimental initial local buckling strength of steel plates with imperfections so that theoretical predictions using the novel method can be compared with test results.

11. CONCLUSIONS

A theoretical study on the post-local buckling behaviour of steel plates in concrete-filled welded thin-walled box columns has been presented in this paper by undertaking a geometric and material nonlinear finite element analysis. The effects of various geometric imperfections, residual stresses and width-to-thickness ratios on the post-local buckling strength of clamped steel plates restrained by concrete have been demonstrated. The initial local buckling loads and the post-local buckling reserve strength of plates with imperfections can be determined efficiently from a theoretical analysis by using the novel method developed in this study. The accuracy of the design models has been verified by a classical solution and experimental results. The proposed effective width formulas can be used in the ultimate strength calculation of short thin-walled concrete filled box columns in compression. Further research is needed to investigate the experimental initial local buckling loads of steel plates with imperfections in concrete-filled box columns.

REFERENCES

1. Levy, S., Buckling of rectangular plates with built-in edges. *Journal of Applied Mechanics,* 1942, December, A171-174.

2. Coan, J.M., Large deflection theory for plates with small initial curvature loaded in edge compression. *Trans. Am. Soc. Mech. Engrs,* 1951, **73**, 143-162.

3. Yamaki, N., Postbuckling behaviour of rectangular plates with small initial curvature loaded in edge compression. *J. Appl. Mech. Am. Soc. Mech. Engrs*, 1959, **26**, 407-414.

4. Crisfield, M.A., Full-range analysis of steel plates and stiffened plating under uniaxial compression. *Proc. Instn. Civ. Engrs, Part 2,*1975, **59**, 595-624.

5. Little, G.H., Collapse analysis of plates with strain hardening. *Int. J. Mech. Sci.*, 1981, **23**(9), 561-576.

6. Mofflin, D. S. and Dwight, J. B., Buckling of aluminium plates in compression. In *Behaviour of Thin-Walled Structures*, Edited by Rhodes, J. and Spences, J., Elsevier Applied Science Publishers Ltd, 1984, 399-427.

7. Ge, H.B. and Usami, T., Strength of concrete-filled thin-walled steel box columns: experiment. *Journal of Structural Engineering*, 1992, **118**(11), 3036-3054.

8. Ge, H.B. and Usami, T., Strength analysis of concrete-filled thin-walled steel box columns. *Journal of Constructional Steel Research*, 1994, **30**, 259-281.

9. Wright, H. D., Buckling of plates in contact with a rigid medium. *The structural Engineer*, 1993, **71**(12), 209-215.

10. Wright, H. D., Local stability of filled and encased steel sections. *Journal of Structural Engineering*, 1995, **121**(10), 1382-1388.

11. Bridge, R.Q., O'Shea, M.D., Gardner, P., Grigson, R. and Tyrell, J., Local buckling of square thin-walled steel tubes with concrete infill. *Proceedings of the International Conference on Structural Stability and Design*, Sydney, Australia, 1995, 307-314.

12. Uy, B. and Bradford, M.A., Local buckling of thin steel plates in composite construction: experimental and theoretical study. *Proc. Instn. Civ. Engrs Structs & Bldgs*, 1995, **110**, 426-440.

13. Uy, B. and Bradford, M.A., Elastic Local buckling of thin steel plates in composite steel-concrete members. *Engineering Structures*, 1996, **18**(3), 193-200.

14. STRAND6.1, *Reference Manual and User Guide*, G+D Computing Pty Ltd, Sydney, Australia, 1993.

15. Dwight, J.B., Prediction of residual stresses caused by welding. *Steel Construction*, 1975, **9**(1), 2-9.

16. Ramberg, W. and Osgood, W.R., Description of stress-strain curves by three parameters. *NACA Technical Note*, No. 902, 1943.

17. Bulson, P.S., *The Stability of Flat Plates*, Chatto and Windus, London, 1970.

18. Walker, A.C., A brief review of plate buckling research. In *Behaviour of Thin-Walled Structures*, Edited by Rhodes, J. and Spences, J., Elsevier Applied Science Publishers Ltd, 1984, 375-397.

19. Liang, Q.Q. and Uy, B., Parametric study on the structural behaviour of steel plates in concrete-filled fabricated thin-walled box columns. *Advances in Structural Engineering*, 1998, **2**(1), 57-71.

20. Uy, B., Local and post-local buckling of concrete-filled steel welded box columns. *Journal of Constructional Steel Research*, 1998, **47**, 47-72.

Figures and Tables

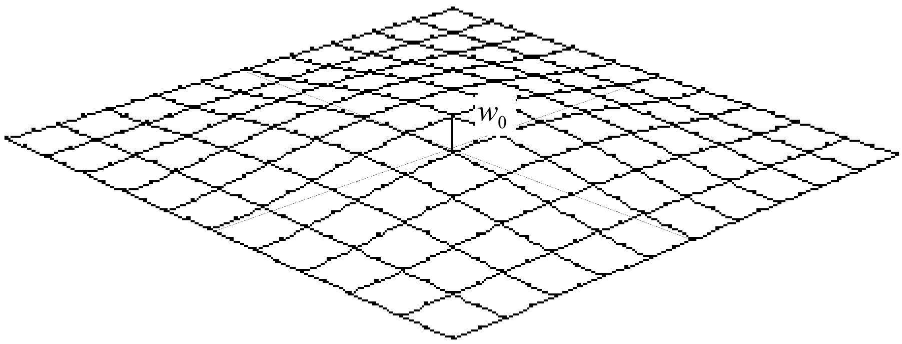

Fig. 1. Initial geometric imperfection of clamped plate

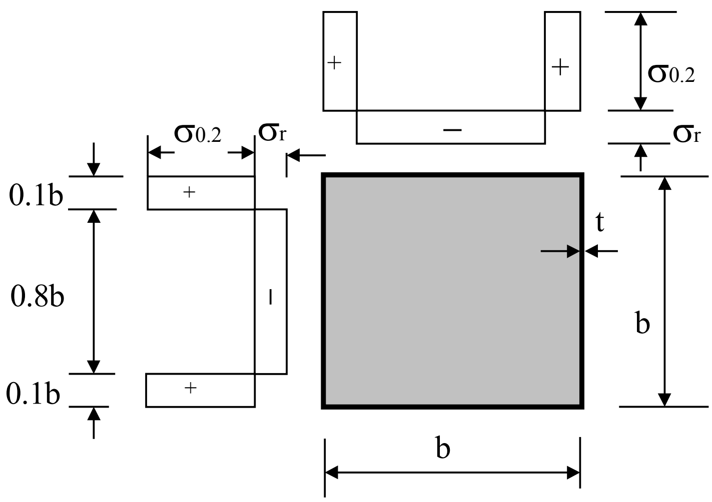

Fig. 2. Residual stress pattern for concrete-filled welded steel box columns

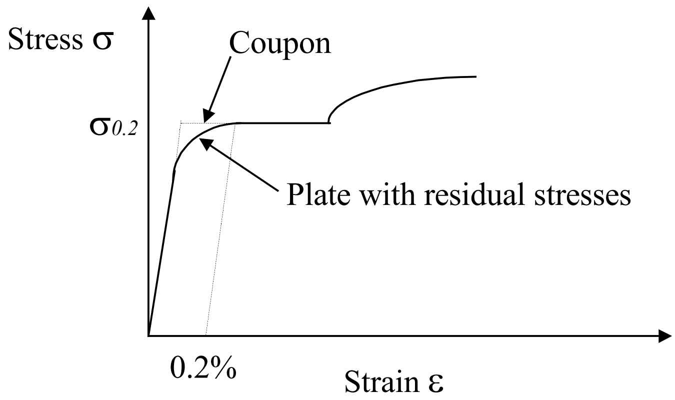

Fig. 3. Material stress-strain curve of steel plates with residual stresses

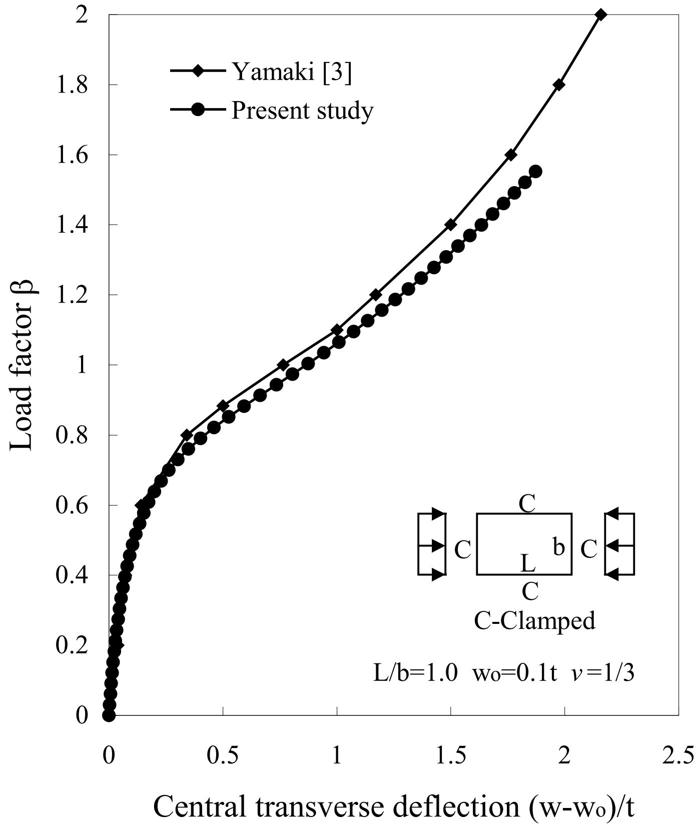

Fig. 4. Comparison of present study with Yamaki's solution

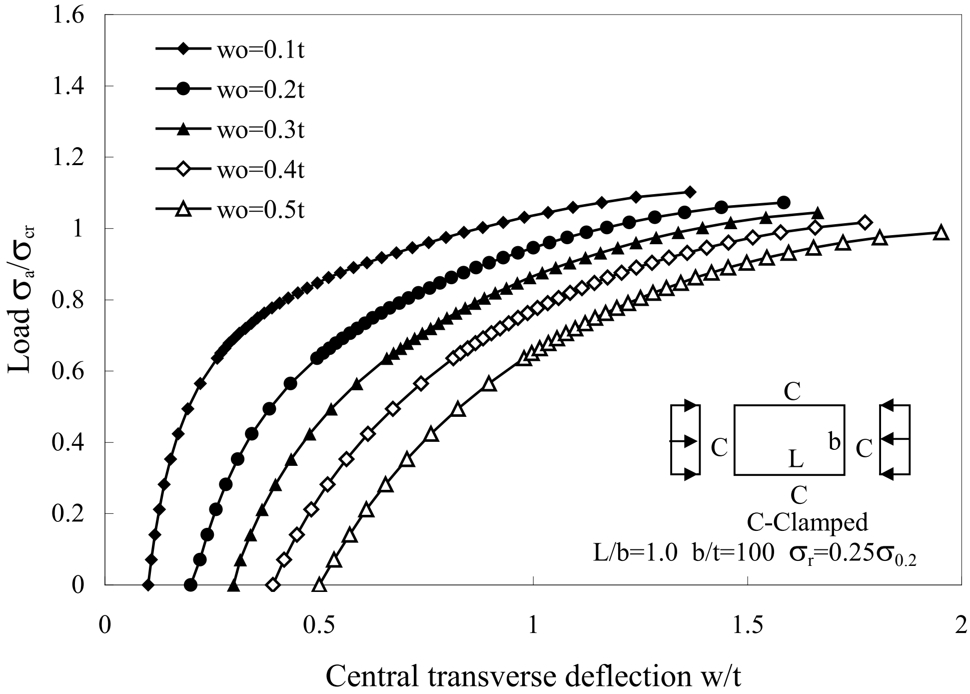

Fig. 5. Load-transverse deflection curves of plates

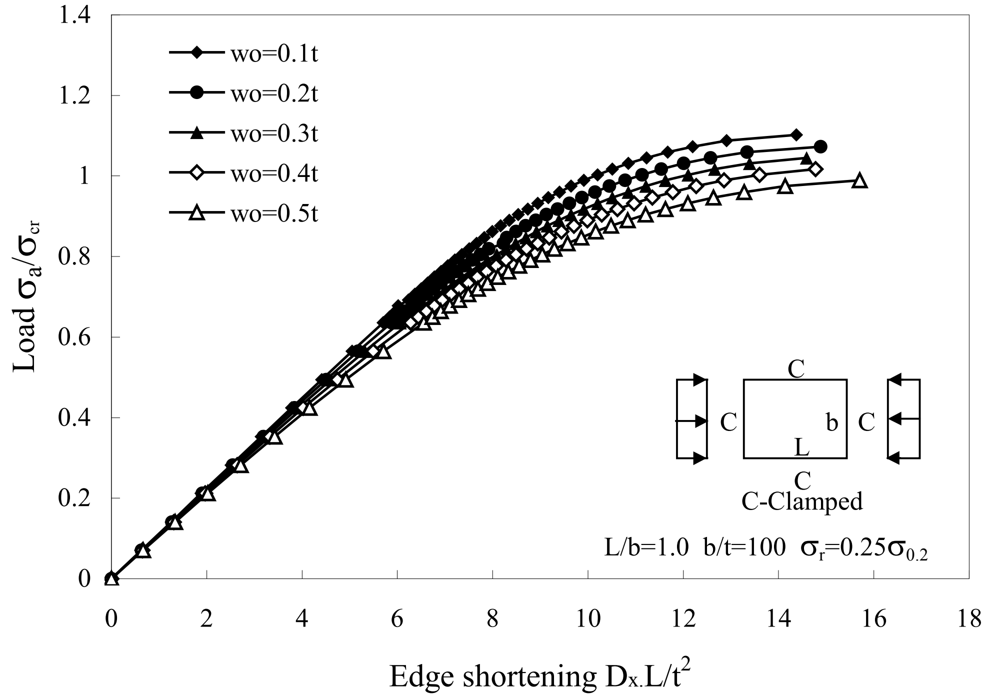

Fig. 6. Load-edge shortening curves of plates

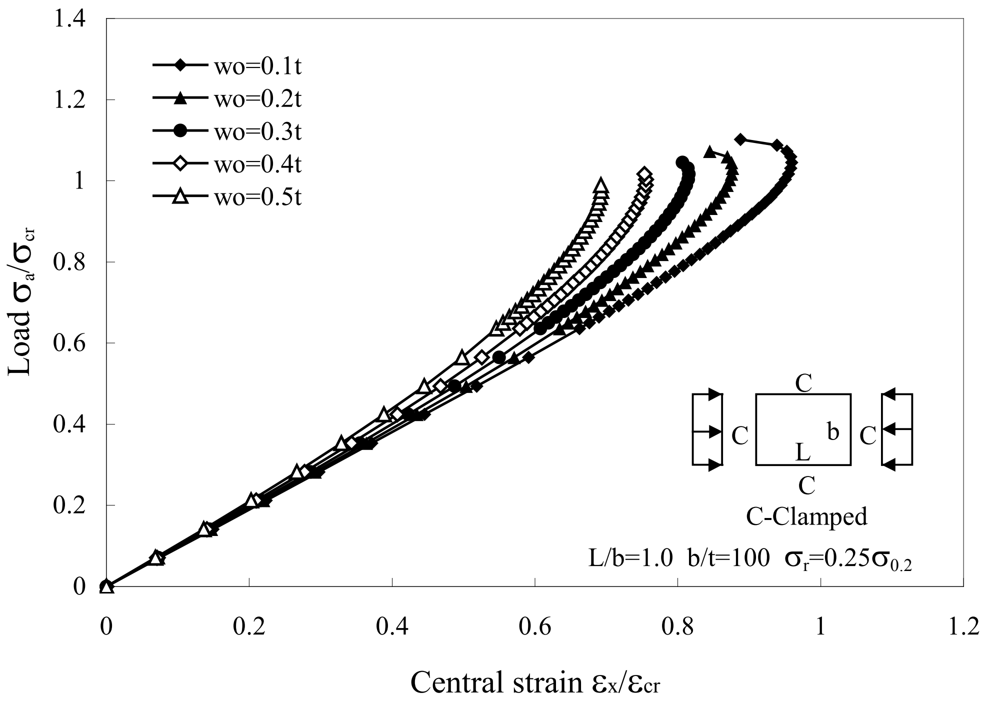

Fig. 7. Load-strain curves of plates

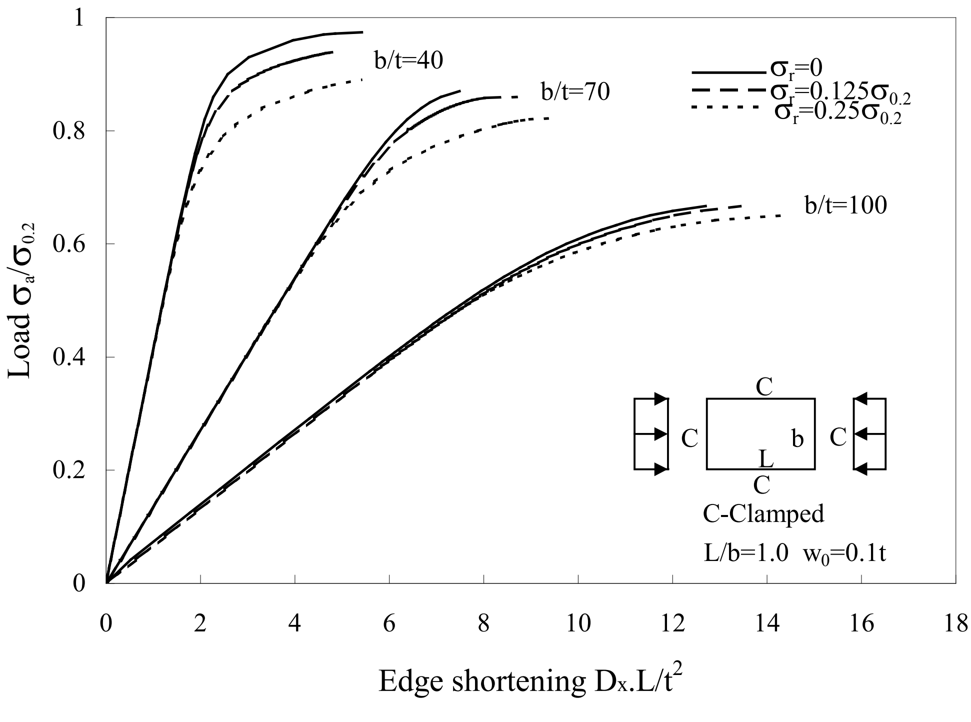

Fig. 8. Effects of residual stresses on load-edge shortening curves of plates

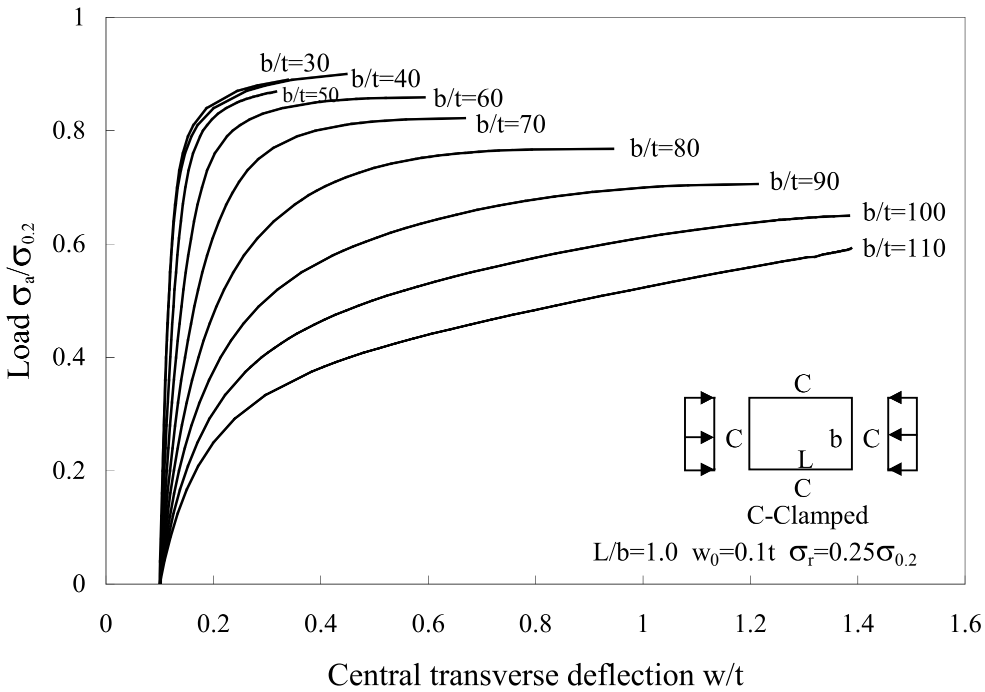

Fig. 9. Load-transverse deflection curves of plates with various b/t ratios

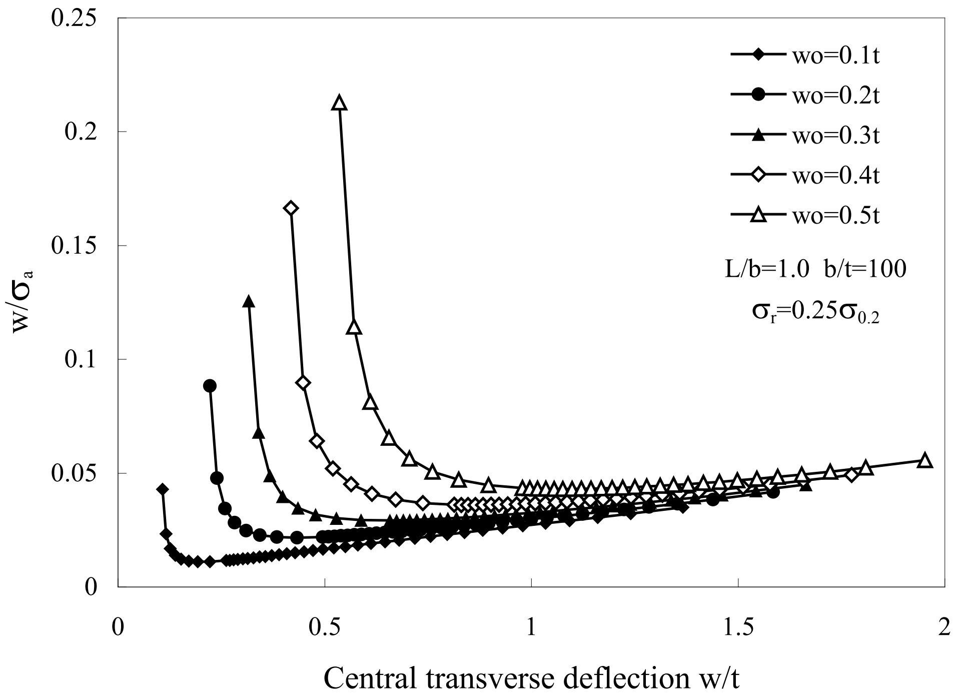

Fig. 10. Load-deflection plots for determining initial buckling loads of plates

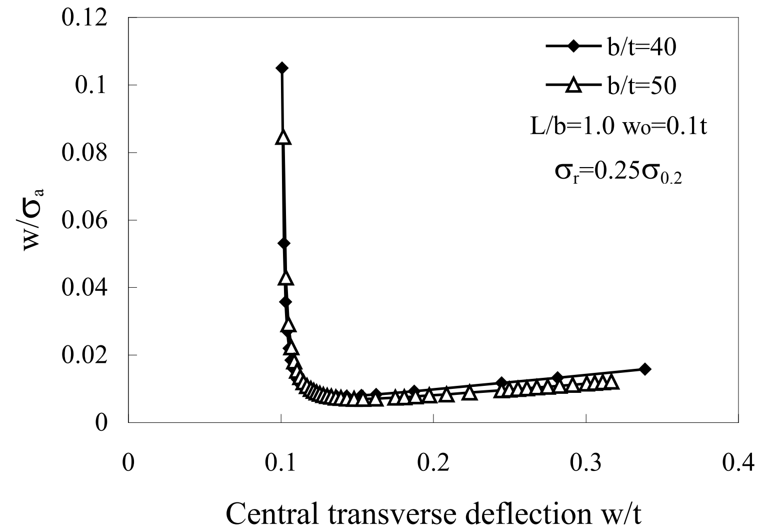

Fig. 11. Load-deflection plots for determining initial buckling loads of plates

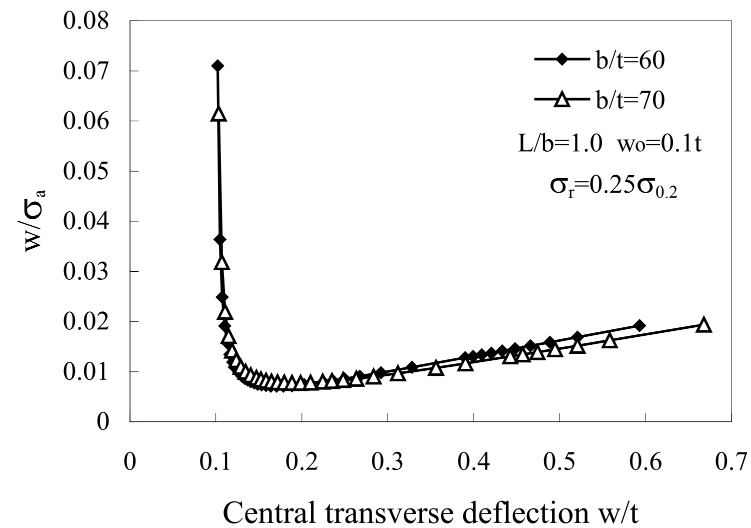

Fig. 12. Load-deflection plots for determining initial buckling loads of plates

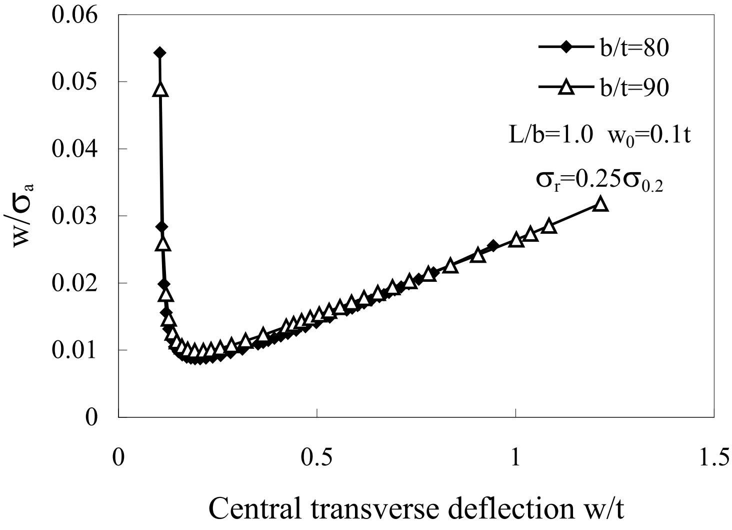

Fig. 13. Load-deflection plots for determining initial buckling loads of plates

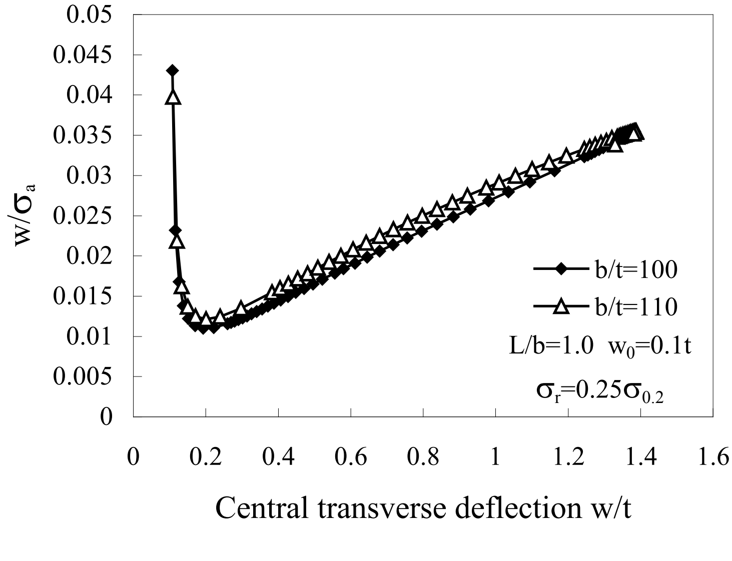

Fig. 14. Load-deflection plots for determining initial buckling loads of plates

Table 1 Local and post-local buckling strength of steel plates with imperfections

w_0 / t	$(w/\sigma_a)_{\min}$ (mm/MPa)	w/t	t (mm)	σ_c (MPa)	σ_P (MPa)	σ_u (MPa)	$\frac{\sigma_P}{\sigma_u}(\%)$
0.1	0.011	0.193	5	87.727	107.273	195	55
0.2	0.022	0.433	5	98.409	91.591	190	48
0.3	0.029	0.658	5	113.448	71.552	185	39
0.4	0.036	0.865	5	120.139	59.861	180	33
0.5	0.043	1.076	5	125.116	49.884	175	28

Table 2 Local and post-local buckling strength of steel plates with imperfections

b/t	$(w/\sigma_a)_{\min}$ (10^{-1}mm/MPa)	w/t (10^{-1})	t (mm)	σ_c (MPa)	σ_P (MPa)	σ_u (MPa)	$\frac{\sigma_P}{\sigma_u}(\%)$
40	0.078	1.367	12.5	219.071	47.929	267	18
50	0.070	1.533	10.0	219.0	41.70	260.7	16
60	0.071	1.706	8.333	200.227	57.473	257.7	22
70	0.077	1.884	7.143	174.772	71.828	246.6	29
80	0.087	1.929	6.250	138.578	91.822	230.4	40
90	0.099	1.917	5.556	107.584	104.216	211.8	49
100	0.110	1.926	5.0	87.545	107.455	195	55
110	0.121	2.004	4.545	75.274	103.226	178.5	58

Table 3 Effective width of steel plates in concrete-filled box columns

$\frac{b}{t}$	σ_{cr} (MPa)	b_e / b (Finite Element Results)	Equation (6) ($\sigma_{cr} > \sigma_{0.2}$)	Equation (5) ($\sigma_{cr} \le \sigma_{0.2}$)
30	1969	0.9	0.872	
40	1108	0.89	0.845	
50	709	0.869	0.814	
60	492	0.859	0.78	
70	361.5	0.822	0.748	
80	276.8	0.768		0.657
90	218.7	0.706		0.607
100	177	0.65		0.566
110	146.4	0.595		0.53

Table 4 Comparison of theoretical predictions with experimental results

Specimen	Size $b \times b$	f_y (MPa)	E (10^3 MPa)	f_c (MPa)	b/t	b_e / b Theory	$N_{uTheory}$ (kN)	N_{uTest} (kN)	$\frac{N_{uTheory}}{N_{uTest}}$
B29	280×280	282	199.4	NA	130.7	0.483	326.8	364.2	0.897
B5	200×200	282	199.4	NA	93.4	0.604	291.6	311.8	0.935
B20	160×160	282	199.4	NA	74.7	0.74	286.2	269	1.063
B17	120×120	282	199.4	NA	56	0.799	231.5	265.5	0.873
B16	80×80	282	199.4	NA	37.4	0.856	165.3	185	0.894
NS1	186×186	294	200	33.6	60	0.783	1428.6	1555	0.919
NS5	186×186	281	200	NA	60	0.787	483.5	517	0.935
NS7	246×246	292	200	40.6	80	0.663	2548.8	3095	0.824
NS11	246×246	292	200	NA	80	0.663	561	563	0.996
NS13	306×306	281	200	44	100	0.579	3953.3	4003	0.988
NS14	306×306	281	200	47	100	0.579	4182.8	4253	0.983
NS15	306×306	281	200	47	100	0.579	4182.8	4495	0.931
NS16	306×306	281	200	47	100	0.579	4182.8	4658	0.898
NS17	306×306	281	200	NA	100	0.579	587.3	622.3	0.944
Mean									0.934